

## **Impact of the Precipitation State on Texture Evolution during Thermomechanical Processing of AA6016**

Christian Bollmann, Stephan Kovacs and Günter Gottstein

Institute of Physical Metallurgy and Metal Physics, RWTH Aachen University, 52056 Aachen, Germany

The current study was conducted to improve the understanding of the influence of the solution / precipitation state on the texture evolution during cold rolling and recrystallization in AA6016. Therefore, three typical solution / precipitation states were distinguished, namely the solution heat treated “SHT”, the peak-aged “PA” and the over-aged “OA” condition. The experimental investigations clearly demonstrate an impact of the precipitation state on the cold rolling and recrystallization textures. The recrystallization textures of the SHT and PA material were fairly similar compared to the OA material. The difference in the formation of the recrystallization textures was attributed to the difference in the involved nucleation mechanism. While nucleation at shear bands was considered as an important nucleation mechanism in the PA material, particle stimulated nucleation (PSN) was the dominant nucleation mechanism in the OA material.

**Keywords:** *recrystallization, texture, nucleation, precipitation*

### **1. Introduction**

The heat-treatable Al-Mg-Si alloys are widely used for automotive applications, especially for automotive panels, since 6xxx series alloys combine excellent formability, good surface appearance and high in-service strength. In order to optimize the formability, the crystallographic texture of the sheet plays an important role as it controls the plastic anisotropy. In particular, it is of importance to understand the formation of recrystallization textures in these alloys [1-3]. In the past, many investigations addressed the influence of the initial texture prior to cold rolling and the amount of applied deformation during cold rolling on the development of recrystallization textures. However, the precipitation state is an additional state variable to control the texture [3, 4]. Hence, the impact of the dissolution / precipitation state on texture evolution during cold rolling and recrystallization was analyzed in detail in this study. For this purpose, three typical solution / precipitation states, namely the solution heat treated “SHT”, the peak-aged “PA” and the over-aged “OA” condition were distinguished. The parameters being varied were the amount of cold rolling and the annealing temperature. The main investigation method was X-ray macrotexture analysis complemented by local texture analysis by means of electron back scatter diffraction “EBSD” in the SEM.

### **2. Experimental procedure**

Samples were taken from a modified hot band of AA6016 which was commercially produced by ALERIS in the framework of the Strategic Research Programme of M2i. Since the goal of this investigation was to achieve a better understanding of the texture evolution in AA6016 depending on the precipitation state, three distinctively different precipitation states were produced by subjecting samples to various annealing treatments.

First, the as-received hot band was solution heat treated (SHT) for 2h at 560°C. Then, the material was directly water quenched and stored in liquid nitrogen in order to prevent any precipitation reaction. At that stage the samples comprised a completely recrystallized structure with slightly elongated grains and a typical recrystallization texture with cube and RD-rotated cube as the major texture components. The second group of samples underwent a typical age-hardening treatment for Al-Mg-Si alloys to obtain a state with finely distributed precipitates. Such a precipitation state is related to the peak-aged (PA) condition. It is usually reached through an additional annealing of the SHT material for 2h at 180°C [5]. A distinctively different precipitation state was produced by slow cooling from 560°C down to 300°C at 2.5K/h and holding at 300°C for several hours [6]. In this way, the third group of samples was over-aged (OA condition) and so, much coarser precipitates than in the PA condition were present in the material. Subsequently, the samples were cold rolled to 75, 87 and 95% thickness reduction on a laboratory rolling mill. Finally, they were annealed at 300, 400 and 500°C for different annealing times.

Pole figures were measured by means of an automated X-ray texture goniometer. From the pole figures  $\{111\}$ ,  $\{002\}$ ,  $\{022\}$  and  $\{113\}$  the orientation distribution functions (ODFs) were calculated. The ODFs were also quantitatively analyzed by calculating volume fractions for different texture components. The different texture components were classified into three typical texture component groups, namely cube components,  $\beta$ -fiber components and all other components (including random components). The texture evolution during recrystallization was also followed by means of scanning electron microscopy (SEM) and electron backscatter diffraction (EBSD).

### 3. Experimental Results

#### 3.1 Texture evolution during cold rolling

After cold rolling, the samples showed slightly different textures as can be seen in Fig. 2. In principle, the textures were composed of the typical fcc rolling texture components C, S and B along the  $\beta$ -fiber where the major texture component varied depending on the solution / precipitation state. While SHT and OA samples showed a maximum intensity close to C at 75% thickness reduction (Fig. 2a), PA samples revealed a maximum intensity between S and B along the  $\beta$ -fiber. Further cold rolling to 87% (Fig. 2b) led again to a maximum intensity near C for OA and a pronounced intensity peak at B for PA. The cold rolling textures after 95% thickness reduction (Fig. 2c) displayed a typical “B-type” texture for PA and SHT samples, whereas OA samples revealed an almost constant intensity along the  $\beta$ -fiber.

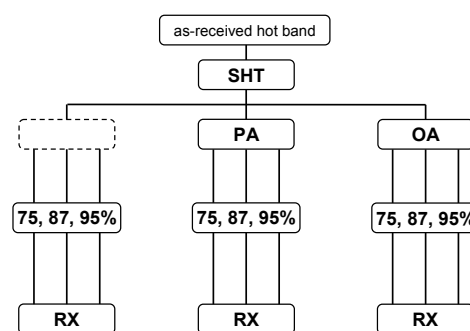


Fig. 1 Schematic diagram illustrating the sequence of main processing steps applied in this study

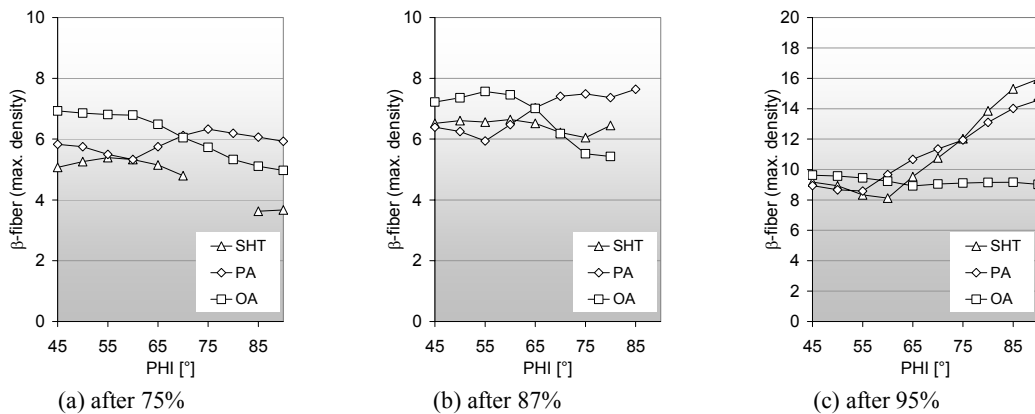


Fig. 2 Cold rolling textures after 75, 87 and 95% thickness reduction for three different solution / precipitation conditions (see Fig. 1); the cold rolling textures are represented by means of the skeleton line along the  $\beta$ -fiber

### 3.2 Texture evolution during recrystallization

To investigate the influence of the precipitation state on the recrystallization texture, the samples were annealed at different temperatures for 1h. As an example, the recrystallization textures after annealing at 400°C for 1h are shown in Fig. 3. They were all composed of a few characteristic recrystallization texture components, e.g. the ideal cube orientation with its ND- and RD-rotations, but they also revealed some distinct differences with regard to specific texture components, e.g. the P-orientation. In fact, the volume fractions of the three texture component groups undoubtedly showed an influence of the precipitation state on the recrystallization textures. In general, the SHT and PA samples displayed fairly similar textures compared to the OA sample. At low and medium deformation degrees (up to 87%) very weak textures were formed with slight preference of the ideal cube orientation. The SHT and PA samples showed a strong scattering of the cube orientation around ND and RD, and retained deformation components. The OA samples revealed the lowest maximum intensity, and the P-orientation was found. Taking the volume fraction of the random part as a measure of texture sharpness, the weakest textures developed in the OA samples. At high deformation degrees (95%), recrystallization textures with larger maximum intensities were formed. Here, the cube orientation became more pronounced again and consequently, the fraction of the random part was reduced. However, the P-orientation was more pronounced in the OA condition than in the SHT and PA condition at all rolling reductions.

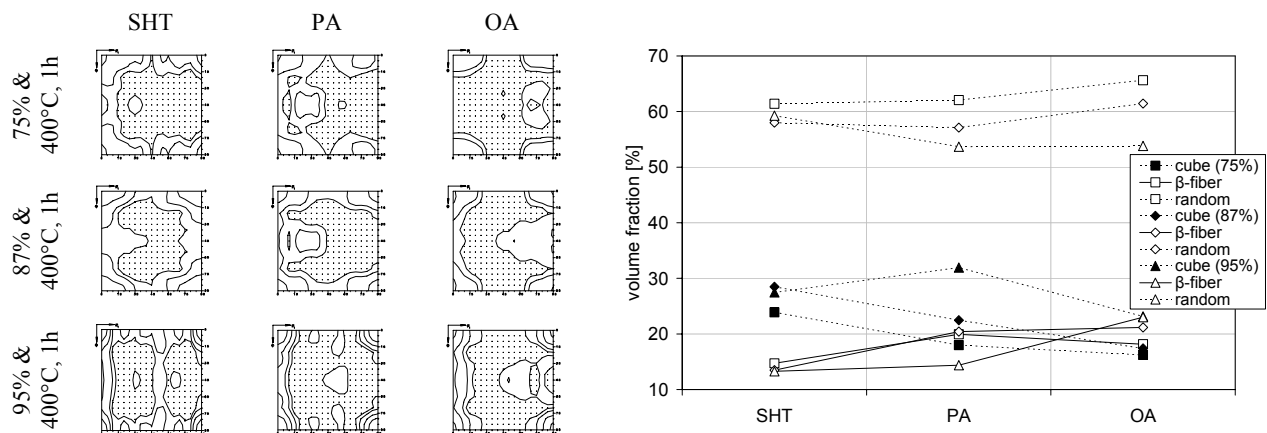


Fig. 3 Recrystallization textures for three different solution / precipitation states achieved after annealing at 400°C for 1h (see Fig. 1); the textures are represented by  $\phi_2 = 0^\circ$  sections (Levels: 1.2 / 2 / 4 / 7 / 12) and in terms of volume fractions for respective texture components

In order to better understand the formation of recrystallization textures and how they depend on the solution / precipitation state, the texture and microstructure evolution during recrystallization was investigated for the PA and OA condition, respectively. Each sample was cold rolled to 75% thickness reduction and annealed at 300°C for various annealing times. A representative area for each sample was analyzed via SEM/ EBSD.

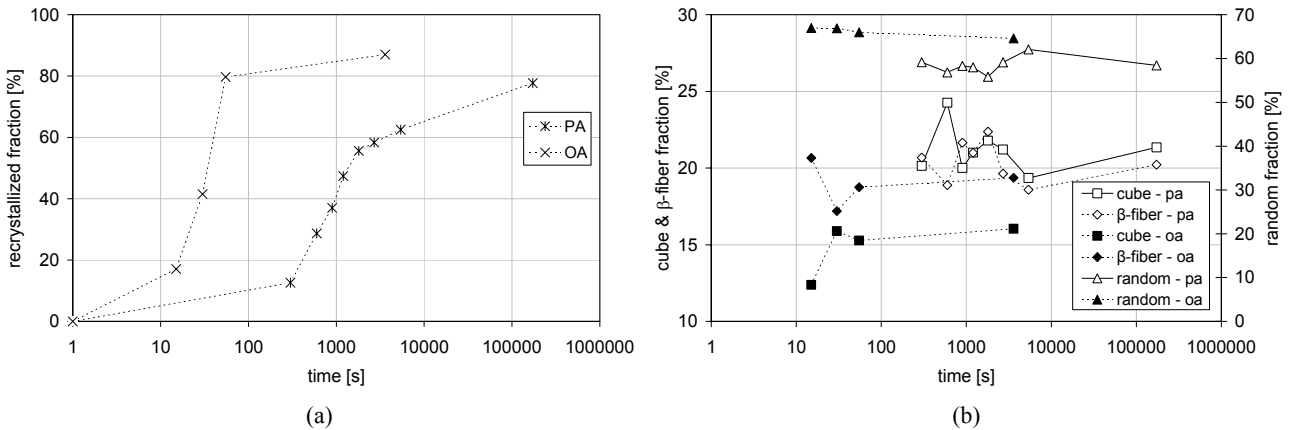


Fig. 4 (a) Recrystallization kinetics from EBSD data for the PA and OA sample which were cold rolled to 75% thickness reduction and annealed at 300°C; (b) texture evolution of recrystallized grains for both material conditions, the textures are represented in terms of volume fractions for respective texture component groups

The recrystallization kinetics were significantly different for both samples as shown in Fig. 4a. While the OA sample was almost completely recrystallized after annealing for 1min, it took several hours for the PA sample (48h to reach  $X = 80\%$ ). The texture evolution of recrystallized grains only was analyzed as shown in Fig. 4b. The results revealed a significant difference in the nuclei spectra between both material states. The fraction of the random part was about 10% larger for OA compared to PA and conversely, the cube fraction was lower by the same amount. Besides, the initial orientation spectrum of recrystallized grains was more or less unchanged upon recrystallization for PA (Fig. 4b).

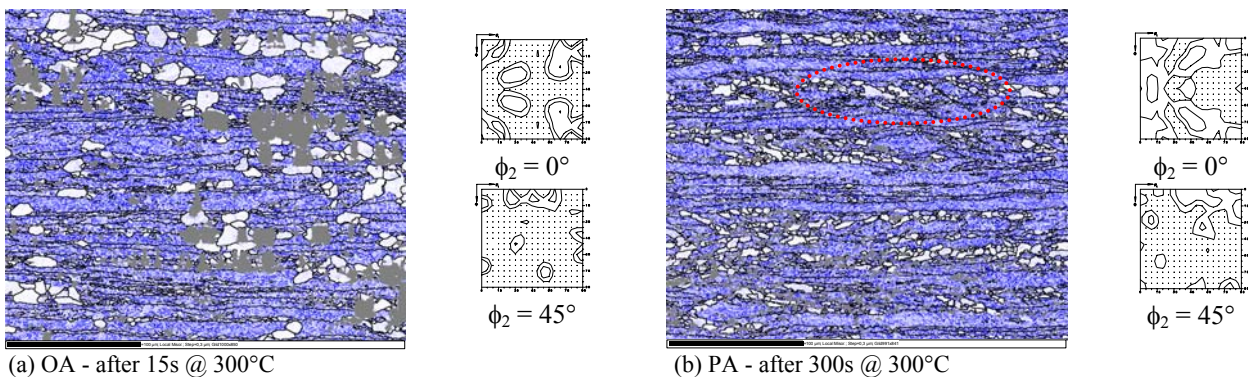


Fig. 5 Partially recrystallized microstructures and corresponding ODFs of recrystallized grains only: (a) over-aged condition, (b) peak-aged condition

The deformation microstructures of both materials were found to be dissimilar. While in the PA sample shear bands were observed, they were not found in the OA sample. After 300s annealing of the PA sample at 300°C, the first recrystallized grains were also observed in these shear bands (Fig. 5b). The corresponding ODF of the recrystallized grains displayed some typical texture components related to shear band nucleation, e.g. G- and Q-orientation. In the OA sample, the first recrystallized grains were observed close to large particles (grey colored areas in Fig. 5a).

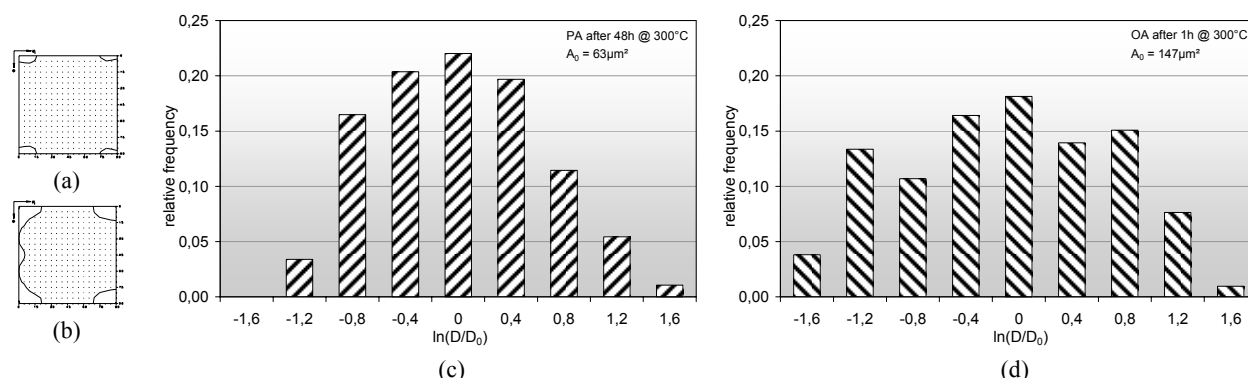


Fig. 6 (a) Experimental recrystallization texture for OA material after 75% cold rolling and annealing at 400°C for 1h, (b) corresponding simulated recrystallization texture; the textures are represented by  $\phi_2 = 0^\circ$  sections (Levels: 2 / 4); experimental size distribution of recrystallized grains: (c) for PA after 48h at 300°C and (d) for OA after 1h at 300°C

The experimental size distributions of recrystallized grains for PA and OA at  $X \approx 80\%$  (Fig. 6c,d) revealed slight differences as well. The size distribution for the OA material was broader compared to the PA material. The recrystallization textures for the OA material were also simulated assuming  $\pm 40^\circ$   $\langle 111 \rangle$  growth selection out of a random nucleus spectrum for the corresponding deformation textures. In this way, the experimental recrystallization textures for the OA material were reproduced (Fig. 6a,b).

#### 4. Discussion

The experimental observations clearly demonstrate an influence of the solution / precipitation state on the cold rolling textures. For a wider range of rolling reductions, it was shown that OA samples tend to comprise a “C-type” texture, whereas PA samples tend to a “B-type” texture (Fig. 2). For SHT samples, the type of texture changes from “C-type” to “B-type” texture at large rolling reductions. The underlying reason for the observations is certainly found in the different microscopic deformation behaviour for the respective precipitation states. While shear bands were observed in the deformation microstructure in the PA material after only 75% cold rolling reduction (Fig. 5b), they were not found in the OA material. From these observations the occurrence of the “B-type” texture must be correlated to the formation of shear bands. Similar results were obtained for Al-1.8 % Cu by Engler et. al. [7] but the underlying reason was not yet fully understood. However, the formation of shear bands also resulted in a strong B-orientation. In the OA sample, a cold rolling texture similar to pure Al [8] was observed. Hence, it was concluded that the “C-type” texture in the OA condition is due to more homogeneous deformation compared to the PA condition. Thus, the slip occurs closer to FC-model which predicts a stable orientation near C [7].

The experimental investigations also demonstrate a significant impact of the precipitation state on the process of recrystallization and thus, on the development of the recrystallization textures. The recrystallization textures of the SHT and PA material were fairly similar compared to the OA material (Fig. 3). In summary, the OA material revealed the largest volume fraction of random orientations and the lowest amount of cube orientations. Moreover, specific texture components, e.g. the P-orientation, were much more pronounced in this material. This fact already indicates a difference in the contribution of the respective potential nucleation mechanisms during recrystallization between SHT and PA versus OA.

In order to better understand the formation of the recrystallization texture for the PA and OA material, the microstructure evolution during recrystallization was studied for both materials. The analysis of the OA material revealed that the first recrystallized grains were observed at large particles where accelerated nucleation (particle stimulated nucleation, PSN) is likely to take place in the deformation zones around these particles [9,10]. Furthermore, the recrystallization textures also displayed typical texture components, e.g. the P-orientation, which are related to PSN. Due to the fact

that the experimental recrystallization textures could be reasonably well reproduced by simulations (Fig. 6a,b) the dominance of PSN for OA material is strongly underlined by this study. In the PA material, shear bands were formed during cold rolling. During recrystallization, first recrystallized grains were observed at these shear bands (Fig. 5b) and the corresponding ODF comprised some typical orientations related to shear band nucleation, e.g. G- and Q-orientation. Hence, it is concluded that shear band nucleation is the dominant nucleation mechanism in the PA material. Further, the orientation spectrum that developed during initial stages of recrystallization (Fig. 5b) remained essentially unchanged during recrystallization (Fig. 4b) and thus, it determined the final recrystallization textures. This supports a strong influence of “oriented nucleation” or early stage “growth selection” on the formation of recrystallization textures for the PA material. Most probably, a combination of a growth selection from a limited nucleus orientation spectrum seems to have caused such texture development as also observed in other Al alloys [9].

## 5. Summary

The impact of the solution / precipitation state on the texture evolution during thermomechanical processing was investigated in the alloy AA6016. Three typical solution / precipitation states were distinguished. The experimental investigations clearly demonstrated an influence of the precipitation state on the cold rolling textures. For a wide range of rolling reductions, a “C-type” texture was observed for the OA condition, while the PA condition showed a “B-type” texture. Moreover, the SHT samples displayed a transition of the texture from “C-type” to “B-type”. The recrystallization textures for the SHT and PA condition were fairly similar compared to the OA condition. For the PA material, it was observed that the initial orientation spectrum determined the final recrystallization texture. Moreover, nucleation at shear bands was found as an important nucleation mechanism for PA. For the OA material, the experimental observations clearly indicated particle stimulated nucleation (PSN) as dominant nucleation mechanism.

## Acknowledgements

The financial support of the M2i is gratefully acknowledged. This research was carried out under project number MC4.05210 in the framework of the Strategic Research Programme of M2i in the Netherlands ([www.m2i.nl](http://www.m2i.nl)).

## References

- [1] J. Hirsch: *Virtual Fabrication of Aluminium Products*, (Wiley-VCH Verlag, Weinheim, 2006).
- [2] G.B. Burger, A.K. Gupta, P.W. Jeffrey, D.J. Lloyd: *Materials Characterization* 35 (1995) 23-39.
- [3] O. Engler, J. Hirsch: *Mater. Sci. and Eng. A336* (2002) 249-262.
- [4] O. Engler, M. Tap, J. Hirsch & G. Gottstein: *Mat. Sci. For.* 217-222 (1996) 405-410.
- [5] A. Perovic et al.: *Scripta Mater.* 41, No. 7 (1999) 703-708.
- [6] S.J. Lillywhite, P.B. Prangnell & F.J. Humphreys: *Mater. Sci. & Tech.* 16 (2000) 1112-1120.
- [7] O. Engler, J. Hirsch & K. Lücke: *Acta Metall.* 37, No. 10 (1989) 2743-2753.
- [8] J. Hirsch: *Untersuchung der primären Rekristallisation und ihrer Mechanismen mit Hilfe der Texturanalyse*, Doctoral Thesis (IMM, RWTH Aachen, 1988).
- [9] O. Engler: *Mater. Sci. Technol.* 12 (1996) 859-872.
- [10] O. Engler, J. Hirsch & K. Lücke: *Acta Metall.* 43, No. 1 (1995) 121-138.